Original Article
Food Science and Technology

ISSN 0101-2061 (Print)
ISSN 1678-457X (Online)

DOI: https://doi.org/10.1590/fst.85622

Effects of catalpa seed oil and pomegranate seed oil on body weight and intestinal flora in mice

Jihui WANG[1], Xiangyu CHEN[1], Han WANG[2], Shan XIAO[1], Bo WANG[1], Yanxue CAI[1*]

Abstract

This study investigated the effects of different concentrations of catalpa seed oil (CSO) and pomegranate seed oil (PSO) on body weight and intestinal flora in mice. The results showed that the addition of 10% w/t CSO or PSO had a more significant effect than control (soybean oil) on reducing the body mass index of mice, which was reduced by 24.94% ± 0.08% ($p < 0.01$) and 25.88% ± 0.11% ($p < 0.01$), respectively. Histological observations indicated that no significant changes in the development and structure of mouse intestinal tissue were detected as a result of CSO and PSO. Using bioinformatics technology, CSO and PSO were used to study the clustering of operational taxonomic units and the relative abundance of microorganisms in intestinal bacteria. The analysis found that both functional lipids could reduce the relative abundance of γ-Proteobacteria. It is suggested that CSO and PSO have a regulatory effect on the structure of intestinal microflora in mice. The development reported in this paper provided theoretical support for the functional research and in-depth development of CSO and PSO.

Keywords: catalpa seed oil; pomegranate seed oil; body weight; intestinal flora.

Practical Application: This work will help us understanding the effect of catalpa seed oil and pomegranate seed oil on the structure of intestinal microflora and their application in the functional food.

1 Introduction

Functional oils and fats have been a research hotspot of special dietary products and prepared foods because they contain a variety of special biologically active substances, which have the functions of anti-oxidation, anti-inflammatory, and supplementation of trace elements. Among them, conjugated linolenic acid (CLnA), as an important functional factor in functional oils, has a variety of isomers, including α-eleostearic acid, punicic acid, catalpic acid, and α-gold calendula acid (Yuan et al., 2014). Some researchers compared the effects of linolenic acid and CLnA on lipid metabolism in mice and found that CLnA can upregulate the expression of peroxisome proliferator-activated receptor α (PPARα) (Cho et al., 2011). Among them, research on pomegranate seed oil (PSO) and punicic acid found that PSO can improve insulin sensitivity (Harzallah et al., 2016), and upregulate obesity-mediated hepatic insulin receptor phosphorylation Tyr-972, p-IRB tyr1146, and pAMPK (Raffaele et al., 2020), as well as other mechanisms to prevent obesity. PSO can also reduce low-density lipoprotein cholesterol (LDL-C) and total cholesterol content in blood lipids in mice (Coronado-Reyes et al., 2022; Shagholian et al., 2019).

Changes in the gut microbiota are closely related to the development of obesity (Kim et al., 2019). Numerous studies have shown that an unbalanced intestinal flora structure can affect the host's metabolic and circulatory systems, and that some bacteria produce excessive amounts of endotoxins that can invade the body through the intestinal wall, cause chronic inflammation, and increase insulin sensitivity and excessive fat. Studies have demonstrated that feeding mice a high-fat, high-sugar diet results in alterations in the ratio of intestinal flora as well as excessive fat storage and unbalanced lipid metabolism (Cai et al., 2005; Mi et al., 2022).

Ingestion of punicic acid-rich PSO reduces omental white adipose tissue weight in obese and hyperlipidemic rats (Szymczyk & Szczurek, 2016). In a study comparing the effects of CLnA and conjugated linoleic acid on fat accumulation in rats, a diet containing a 1% mixture of CLnA isomers reduced the amount of adipose tissue by an amount that was eight times greater than that of conjugated linoleic acid (Shagholian et al., 2019). In addition, the weight of perirenal adipose tissue in mice fed genetically modified rapeseed oil containing PSO or punicic acid for 4 weeks decreased in a dose-dependent manner (Demizieux et al., 2016). Furthermore, dietary supplements containing PSO improved high fat diet-induced obesity and insulin resistance in mice, independent of changes in food intake and energy expenditure (Zhang et al., 2017). Some literature also reported that CSO had a specific inhibitory effect on fat storage in high-fat-diet mice (Rachid et al., 2018).

Obesity is associated with gut microbiota abundance and composition (Zacarías et al., 2018). Gut microbiota diversity and

Received 29 July, 2022
Accepted 07 Sept., 2022
[1]*Key Laboratory of Healthy Food Development and Nutrition Regulation of China National Light Industry, School of Life and Health Technology, Dongguan University of Technology, Dongguan, China*
[2]*School of Bioengineering, Dalian Polytechnic University, Dalian, Liaoning, China*
*Corresponding author: Caiyx@dgut.edu.cn

the ratio of relative abundances of *Bacteroidetes* to *Firmicutes* are reduced in obese individuals compared with nonobese individuals (Walters et al., 2014). Some literature reported that *Proteobacteria*, *Bacteroidetes*, and some pathogenic bacteria (such as *Campylobacter* and *Shigella*) increased whereas anti-inflammatory bacteria decreased in obese people (Chatelier et al., 2013). The relative abundance of *Lactobacillus* and *Bifidobacterium* steadily declined as body mass index (BMI) increased, whereas the relative abundance of *Bacteroides* considerably increased (Hou et al., 2020).

PSO and CSO are rich in punicic acid and catalpic acid, which are isomers of CLnA. Studies have shown that functional oils have a regulatory effect on the body weight and intestinal flora of mice (Wang et al., 2019). However, the mechanism of the effect of different CLnA isomers on the body's gut flora is still unclear. In this experiment, PSO and CSO were used as the research objects to analyze their effect on the growth of mice and in a preliminary exploration of the mechanism of their influence on the intestinal flora of mice. This work will provide a new understanding of the effect of functional oils on health. At the same time, it also provides theoretical support for the functional application of PSO and CSO in special dietary foods.

2 Materials and methods

2.1 Materials

CSO and PSO were obtained from Shanghai Yuanye Biological Co., Ltd (Shanghai, China); rabbit anti-mouse PPARα antibody and rabbit anti-mouse PPARγ antibody were purchased from Proteintech (US) Biotechnology Co. (Wuhan, China); horseradish enzyme-labeled goat anti-rabbit IgG and horseradish enzyme-labeled goat anti-mouse IgG were obtained from Bioworld Technology, Inc. (Shanghai, China); GAPDH, PPARα primers were customized from Bao Biotechnology Engineering Co., Ltd (Dalian, China) after checking the Gene Bank.

2.2 Instruments and equipment

PCR Amplifier (T100), Bio-Rad Company, USA; Universal Electrophoresis Instrument Power Supply, Small Vertical Electrophoresis Tank (165-8003), Bio-Rad (Bole) Company, USA; Gel Imaging System (Tanon 6600), Shanghai Tian Neng Technology Co., Ltd; inverted fluorescence phase contrast microscope (IX81), Olympus Corporation; microplate reader, Tecan Austria Co., Ltd; LightCycler 480 II quantitative PCR instrument, Roche Diagnostics (Shanghai) Co., Ltd.

2.3 Experimental mice grouping and experimental design

SPF pure male mice (3-weeks-old) were purchased from the Experimental Animal Center of Dalian Medical University. After a 1-week prefeeding acclimation period, the mice were randomly divided into five groups. The 7% oil content of the standard formula of rat food was increased to 20% as a high-fat-diet ratio. Soybean oil was the normal growth oil of mice. According to the feed ratio (Table 1), it was divided into a control group, 5% w/t, and 10% w/t glutinous rice. The tree seed oil group and the 5% w/t and 10% w/t PSO groups were reared in separate cages for another 7 weeks in the same environment. After the 7-week rearing period, the glucose tolerance of the mice was determined using the IP GTT method, blood was collected from the eyeballs, and the mice were sacrificed by cervical dislocation for dissection. For use, the blood was refrigerated for 0.5 h, centrifuged at 3000 rpm for 15 min, divided into serum and red blood cells, and stored at –80 °C for use.

Table 1. Test mouse diet ratio (100 g).

Group	Fat-free feed (g)	Soybean oil (g)	CSO (g)	PSO (g)
Control	80	20	-	-
5%-CSO	80	15	5	-
10%-CSO	80	10	10	-
5%-PSO	80	15	-	5
10%-PSO	80	10	-	10

2.4 Determination of growth indicators

Body weight and tail length were used as general indicators of mouse growth. After the adaptation period, the initial body weight and tail length of the mice were measured, and then every 7 days until the end of the experiment.

2.5 Determination of BMI

The BMI value depends on the weight and height, the specific formula is as follows, there are at least three mice in each group, and the results are calculated and recorded in detail (Equation 1).

$$\mathrm{BMI} = \frac{\text{Body weight (kg)}}{\text{Tail length}^2\ \text{(mm)}} \quad (1)$$

2.6 Fecal sample collection and storage

The mixed fecal samples of each group of mice raised for 10 weeks after the end of the experiment were collected in a 5 mL sterile centrifuge tube, and the total amount was greater than 0.5 g, and immediately stored in a –80 °C ultralow temperature refrigerator. The fecal samples were used for DNA extraction and detection, avoiding repeated freezing and thawing.

2.7 Preparation of mouse intestinal tissue paraffin sections

A small amount of fresh intestinal tissue was fixed with 10% formaldehyde solution for 24 h; after fixation, the tissue was properly trimmed with a scalpel in a ventilated place, placed in a dehydration box, and subjected to gradient dehydration: 75% ethanol, 4 h; 80% ethanol, 2 h; 95% ethanol, 1 h; 100% ethanol (I), 30 min; fresh 100% ethanol (II), 30 min; transparent: ethanol + xylene equal proportion mixture, 10 min; xylene (I), 30 min; fresh xylene (II), 30 min; infiltration: xylene + paraffin equal proportion mixture, 60 min; paraffin (I), 6 h; fresh paraffin (II), 12 h, 62 °C. Embedding and slicing: Put the tissue dipped in wax into a mold with a layer of hot semiliquid paraffin at the bottom, place it on a cold table to cool completely, pour sufficient paraffin to submerge the tissue, and immediately press the net.

After being completely cooled, slice, try to keep the tissue intact when slicing, and the slice thickness is about 4 μm.

2.8 Hematoxylin-eosin (HE) staining

The paraffin sections of the small and large intestine tissues in this experiment were deparaffinized to a water state with a series of consecutive steps of xylene and graded ethanol to prepare for staining. The steps were as follows: the sample was soaked by xylene (I) for 20 min and new xylene (II) for other 20 min, 100% ethanol, 95% ethanol, 80% ethanol, and 75% ethanol were soaked for 2 min according to the concentration from high to low, and the xylene was thoroughly leached, and then washed with distilled water for 2 min. Immerse in the hematoxylin staining solution for 5 min to examine the effect of hematoxylin staining under a microscope, and then rinse the unbound hematoxylin staining solution slightly with tap water; differentiate with hydrochloric acid and ethanol for 30 s, during this period, lift the sections out of the liquid surface every 5 s; soak in tap water for 15 min; soak in eosin solution for 2 min after soaking up the water, check the eosin staining effect under a microscope; save the stained sections, dehydrate, clear and seal the sections: 95% ethanol (I) and 95% fresh ethanol (II) for 2 min; 100% ethanol (I) and fresh 100% ethanol (II) for 2 min, xylene (I) and fresh xylene (II) for 1 min and then air-dry; add a drop of neutral resin, cover with a cover glass to ensure no air bubbles for sealing, let the neutral resin stand to dry; check the effect by microscopy, and take a photograph.

2.9 16S rRNA sequencing

Amplification of the bacterial 16S rRNA V3 region used the upstream primer (5′-GGTTGTCTCCTGCGACTTCA-3′) and downstream primer (5′-TGGTCCAGGGTTTCTTACTCC-3′). Amplification cycles: GAPDH, 45 cycles; PPARα, 50 cycles. Melt curve parameter setting (1 cycle): 95 °C for 5 s (ramp rate 4.4 °C/s), 60 °C for 1 min (ramp rate 2.2 °C/s), and 95 °C for 5 s (ramp rate 0.11 °C/s). The acquisition mode was continuous, the temperature was cooled to 50 °C for 30 s (ramp rate 2.2 °C/s) for 1 cycle.

2.10 Denaturing Gradient Gel Electrophoresis (DGGE) analysis

DGGE used 8% polyacrylamide gel, the denaturation gradient was 30%-58%. 100% denaturant is defined as containing 40% formamide and 60% of 7 mol/L urea. The running buffer was 1 × TAE, first, pre-electrophoresis was performed at 220 V for 5 min, and then electrophoresis was performed at 85 V for 16 h at a constant temperature of 60 °C. After electrophoresis, silver nitrate staining was performed and photographs were taken. DGGE images were analyzed using Quantity One software. The important differential bands on the DGGE gel were selected for DNA sequencing, and the sequencing results were carried out by Blast comparison with the NCBI Genebank database.

2.11 Statistical analysis

The data are expressed as mean ± standard deviation (χ ± s), analysis of significance was performed using SPSS 19.0 software, and independent-samples *t*-test was used for comparison. In the analysis of comparison results between groups, one asterisk (*) represents $p < 0.05$, two asterisks (**) represent $p < 0.01$, and no significant difference represents $p > 0.05$.

3 Results and analysis

3.1 Body weight, tail length and BMI analysis

After the feeding period, the mice in each group were compared with the original body weight value at the beginning of the experiment and converted into a percentage; the results of calculating the body weight growth are shown in Figure 1a. Through data analysis, it was found that compared with the control group, the weight growth of the CSO and PSO groups

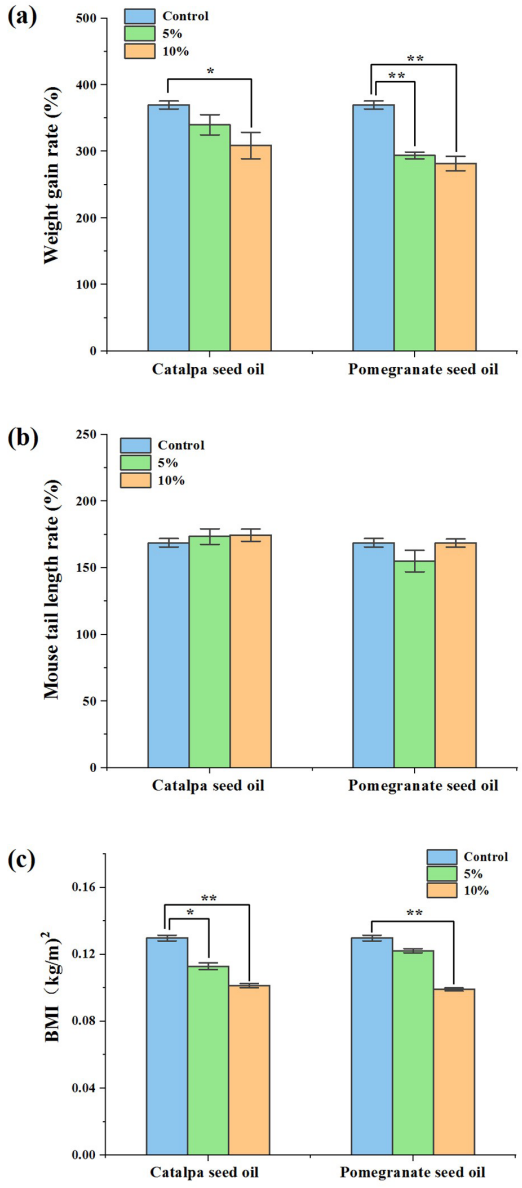

Figure 1. The effects of CSO and PSO on (a) weight gain, (b) tail length, and (c) body mass index (BMI) of mice after 7 weeks of feeding. (* represents $p<0.05$, ** represents $p<0.01$)

(5% PSO group, 10% PSO group and 10% CSO group) decreased by 75.85% ± 1.22%, 88.11% ± 2.23%, and 61.02% ± 1.47%, with significant differences ($p < 0.01$, $p < 0.01$, and $p < 0.05$, respectively). When analyzing the change of body weight, the change of tail length of mice was also analyzed (Figure 1b), and it was found that there was no significant difference in the change of tail length between the CSO and PSO groups compared with the control group ($p > 0.05$).

To intuitively detect the weight changes of mice, the results of BMI analysis are shown in Figure 1c. Compared with the control group, the BMI of mice after consuming functional oils for 7 weeks decreased. Among them, 5% CSO, 10% CSO, and 10% PSO groups were significantly different from the control group ($p < 0.05$, $p < 0.01$, and $p < 0.01$, respectively), which decreased by 16.83% ± 0.04%, 24.94% ± 0.08%, and 25.88% ± 0.11%, respectively, indicating that CSO and PSO had a slowing effect on the weight growth of mice.

3.2 Histomorphological observation of intestine

The gut is the main site of digestion and absorption, and the largest immune organ in the human body. Because of the continuous exposure of the intestinal mucosa to food and microbial antigens, it is normally in a dynamic equilibrium of sustained mild physiological inflammation and immune responses triggered by a large number of antigens (Cicchese et al., 2018; Zou et al., 2021). Abnormal activity of intestinal mucosal immune function or low immune regulation will affect intestinal function (Xu et al., 2014). Both the DNA/RNA in the nucleus and the RNA in the ribosome in the rough endoplasmic reticulum are acidic, and the phosphate backbone of the nucleic acid is negatively charged. These skeletons bind to positively charged basic dyes and dye them purple. Most proteins in the cytoplasm are basic and positively charged. They combine with the negatively charged acid dye eosin and dye them pink. When observing the small intestine tissue of the mice in Figure 2, it was found that the length of the villi and the depth of the crypts in the small intestine of each group were basically similar. Overall, there was basically no significant difference in the integrity and development of the small intestine among the groups. Finally, the results showed that the goblet cells in the colon tissue of the mice in each group were obvious, the villi were dense, and there was no significant difference in histomorphology between the groups. Neither CSO nor PSO had significant effects on the structure of mouse colon tissue. The results showed that CSO and PSO, which are used as edible oils for daily consumption, did not cause adverse changes in intestinal tissue.

3.3 Structure change of intestinal flora in mice

Daily diet and gut microbiota have an important synergistic effect on the regulation of intestinal cellular immune responses. Intestinal flora can affect the human immune system, especially through the intestinal mucosa (Yoo et al., 2020). However, further studies of the interaction between CSO and PSO as well as gut microbiota are required. Through cluster analysis of the operational taxonomic units (OTUs) of the intestinal flora in the control group against the CSO and PSO groups as shown in Figure 3, it was found that 4,098 bacterial species were shared by the five groups of mice, and the other bacterial species were shared or unique to one group. Among them, the control group had 30 unique strains, the 10%-CSO group had 275 unique strains, and the 5%-PSO group had 54 unique strains.

3.4 Relative abundance of intestinal flora in mice

According to the proportion of total microorganisms, the four major phyla in the gastrointestinal tract of humans and mice account for about 99%: *Bacteroidetes*, *Firmicutes*, *Proteobacteria*, and *Actinobacteria* (Turnbaugh et al., 2006). By comparing the differences in the relative abundance of microbial species at the phylum and class levels of the intestinal flora of each group of mice, it was found that in Figure 4a, at the phylum level, *Bacteroidetes*, *Firmicutes*, and *Verrucomicrobia* were three phyla affected by differences in lipids. The phylogenetic tree is shown in Figure 4b. Compared with the control mice (Table 2), the relative abundance ratio of *Bacteroidetes* and *Firmicutes* decreased in the CSO group, whereas the relative abundance of *Bacteroidetes* and *Firmicutes* increased in the PSO group, reflected in *Bacteroides*, *Ruminococcaceae*, and *Oscillibacter* (Figure 4c). Meanwhile, the relative abundance of *Verrucomicrobia* in the CSO and PSO groups was lower than that in the control group, in

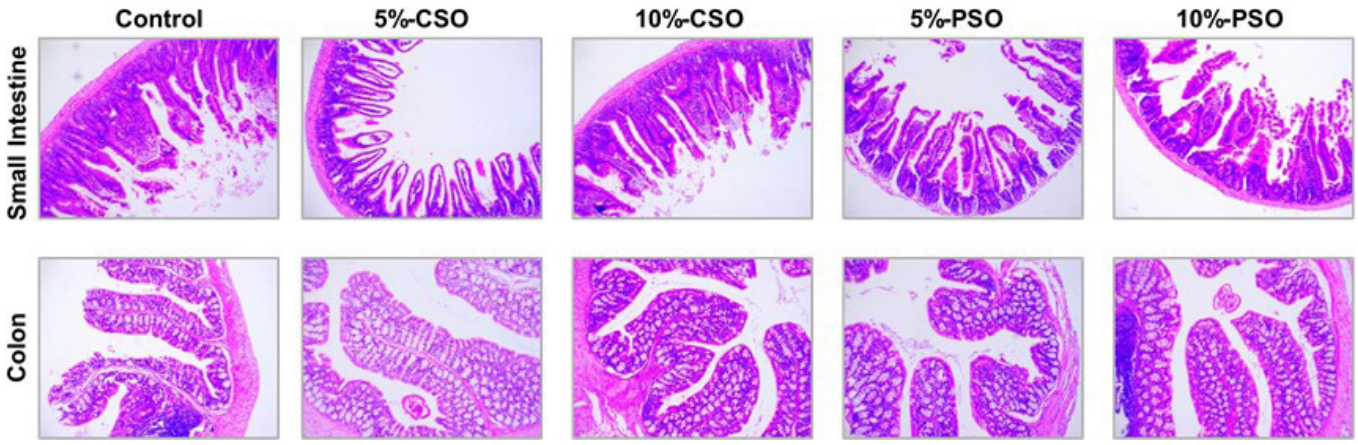

Figure 2. The effects of CSO and PSO on mice's small intestine and colon.

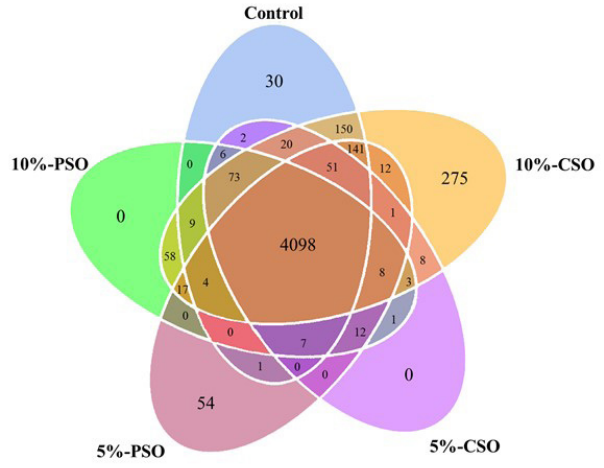

Figure 3. Effect of functional lipids' intake on the intestinal microbial structure.

particular, *Rikenella*, *Clostridiales*, and *Negativibacillus* increased significantly in Figure 4c.

After high-throughput sequencing 16S rRNA sequencing analysis of the composition of the intestinal flora in mice, it was found that at the phylum level, *Firmicutes* and *Bacteroidetes* were the two main phyla, which were coordinated with each other. Many studies have found that high-fat-diet-induced obesity could cause changes in the relative abundance ratio of *Firmicutes* to *Bacteroidetes* at the phylum level of the gut microbiota (Cheng et al., 2017; Wu et al., 2022). Most studies have shown that the relative abundance ratio of *Bacteroidetes* to *Firmicutes* in the intestinal flora of obese individuals was lower than that of nonobese individuals (An et al., 2018). This study found that after 7 weeks of feeding, the ratio of the relative abundance of *Bacteroidetes* to *Firmicutes* increased in the PSO group, consistent with the findings above. However, the relative abundance ratio of *Bacteroidetes* and *Firmicutes* in the intestinal flora of mice

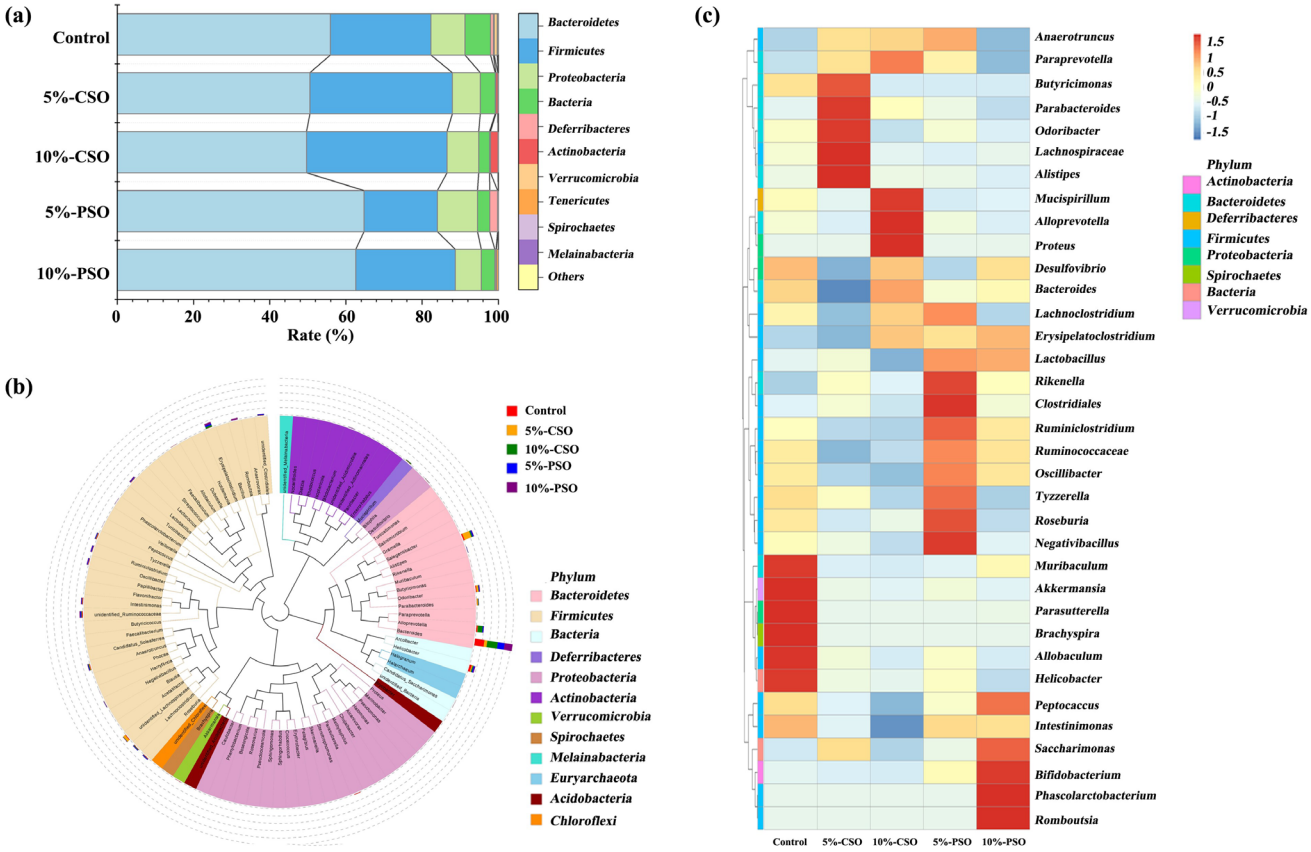

Figure 4. (a) Relative abundance of the top 10 different phyla, (b) phylogenetic tree at the genus level, and (c) heat map of relative abundance at the genus level.

Table 2. Ratio of relative abundance of Bacteroides, Firmicutes, and Verrucomicrobia in intestinal microbes of mice.

Phylum	Control	5%-CSO	10%-CSO	5%-PSO	10%-PSO
Bacteroides (*Bac.*)	0.559	0.505	0.497	0.648	0.626
Firmicutes (*Fir.*)	0.264	0.374	0.368	0.192	0.261
Bac./Fir.	2.118	1.350	1.348	3.368	2.400
Verrucomicrobia	0.007	0.000	0.000	0.001	0.000

in the CSO group decreased. A previous study on this subject found that CSO could upregulate the content of high-density lipoprotein cholesterol (HDL-C) in blood lipids in obese mice, reduce the content of triacylglycerol and LDL-C to improve blood lipid metabolism, and at the same time may regulate the transcription level and protein expression of PPARα. The effects on the regulation mechanism of glucose and lipid metabolism in mice suggest that the weight regulation of CSO in mice may be related to its effects on blood lipids and the transcription level and protein expression of PPARα.

At the class level, as shown in Figure 5a, the relative abundance of γ-Proteobacteria in the CSO and PSO groups was reduced compared with the control group. γ-Proteobacteria contains many important pathogens, such as *Salmonella* (enteritis and typhoid), *Yersinia pestis* (plague), *Vibrio cholerae* (cholera), *Pseudomonas aeruginosa* (hospitalized or pulmonary infection in cystic fibrosis patients), and *Escherichia coli* (food poisoning). In this study, the relative abundance of γ-Proteobacteria was found to be significantly reduced in the CSO and PSO groups (Table 3), and different bacteria of γ-Proteobacteria were species

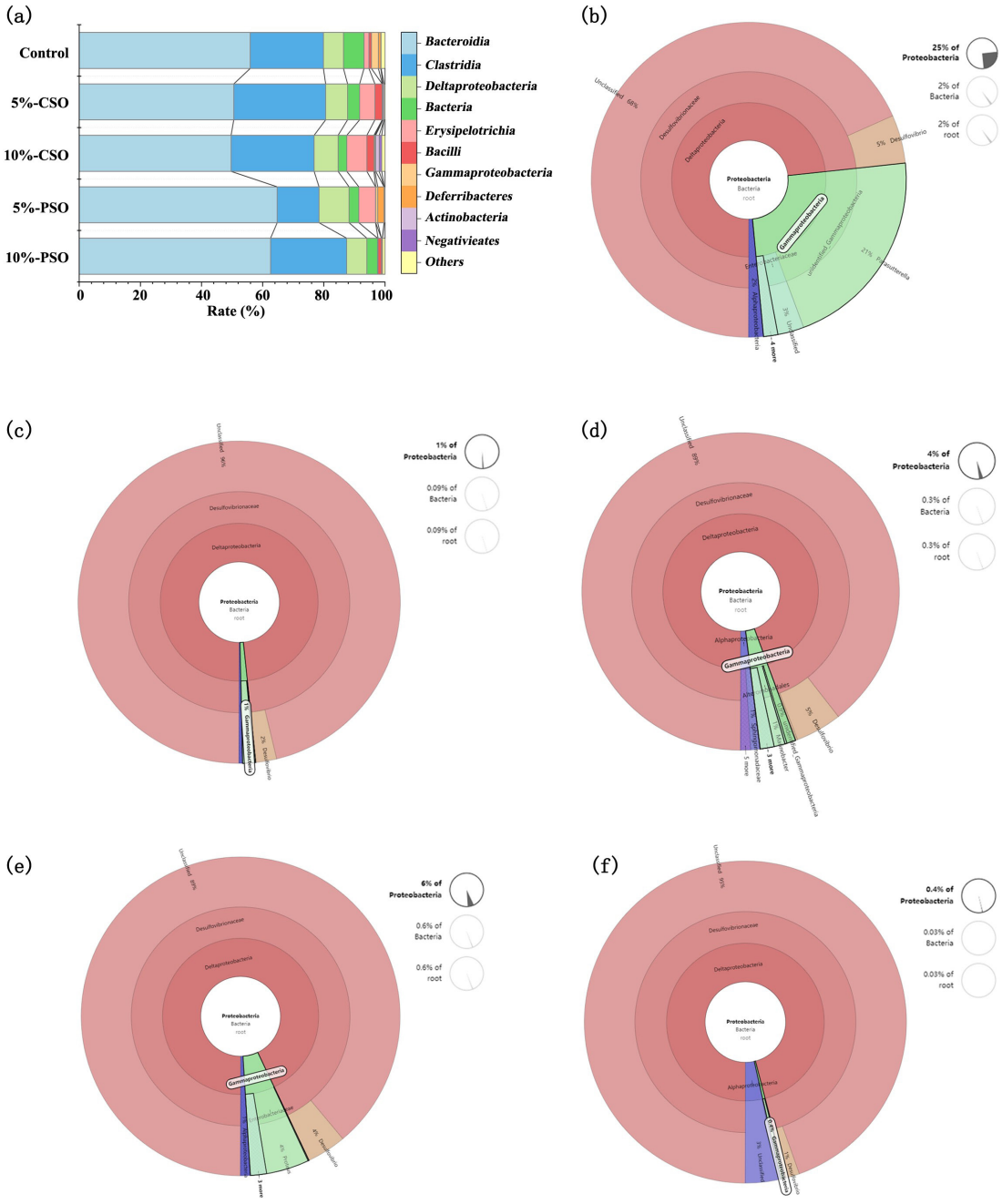

Figure 5. (a) Relative abundance of the top 10 classes and species annotations of γ-Proteobacteria using Krona from (b) control, (c) 5%-CSO, (d) 10%-CSO, (e) 5%-PSO, and (f) 10%-PSO.

Table 3. Relative abundance of the γ-Proteobacteria.

Class	Control	5%-CSO	10%-CSO	5%-PSO	10%-PSO
γ-Proteobacteria	0.022	0.001	0.003	0.006	0.001

annotated using Krona-figure shown in Figure 5b-5f, suggesting that CSO and PSO could improve the harmful microorganisms in the intestinal flora to a certain extent.

Research and statistical analyses have identified distinct bacterial genera in the gut microbiota and their relationship to nutrient intake. The gut microbiota can directly defend against pathogens by inducing the production of antibodies that can strengthen the defense of the host immune system after colonization of the intestinal epithelium, metabolizing indigestible compounds in food, and its role in the gut-brain axis to exert a neurological function (Liu et al., 2022). With growth and development, nutritional changes, fertility, and age, the gastrointestinal flora undergoes a physiological succession (Lozupone et al., 2012), which plays a nonnegligible role in the regulation of body health and energy metabolism.

4 Conclusion

In conclusion, this study found that CSO and PSO could reduce the weight growth of mice, but had no significant effect on the tail length of mice. Compared with the control, 10% CSO and 10% PSO significantly reduced the BMI of mice. The intestinal tissue development and structure were detected with CSO and PSO and there were no significant changes. Through the analysis of OTU clustering of the intestinal flora of mice, the relative abundance changes at the phylum and class levels, it was found that CSO decreased the ratio of abundance of *Bacteroidetes* and *Firmicutes* phyla in the intestinal flora of mice, whereas PSO increased the relative abundance ratio. At the same time, both functional oils could reduce the relative abundance of γ-Proteobacteria, suggesting that CSO and PSO had a regulatory effect on the structure of intestinal flora in mice. This work helped to provide a new understanding of functional studies of CSO and PSO.

Acknowledgements

This work was supported by Natural Science Foundation of Guangdong province (No. 2019A1515010630, 2019A1515111091) and the National Natural Science Foundation of China (No. 31901682).

References

An, Y., Li, Y., Wang, X., Chen, Z., Xu, H., Wu, L., Li, S., Wang, C., Luan, W., Wang, X., Liu, M., Tang, X., & Yu, L. (2018). Cordycepin reduces weight through regulating gut microbiota in high-fat diet-induced obese rats. *Lipids in Health and Disease*, 17(1), 276. http://dx.doi.org/10.1186/s12944-018-0910-6. PMid:30522511.

Cai, D., Yuan, M., Frantz, D. F., Melendez, P. A., Hansen, L., Lee, J., & Shoelson, S. E. (2005). Local and systemic insulin resistance resulting from hepatic activation of IKK-β and NF-κB. *Nature Medicine*, 11(2), 183-190. http://dx.doi.org/10.1038/nm1166. PMid:15685173.

Chatelier, E., Nielsen, T., Qin, J., Prifti, E., Hildebrand, F., Falony, G., Almeida, M., Arumugam, M., Batto, J. M., Kennedy, S., Leonard, P., Li, J., Burgdorf, K., Grarup, N., Jørgensen, T., Brandslund, I., Nielsen, H. B., Juncker, A. S., Bertalan, M., Levenez, F., Pons, N., Rasmussen, S., Sunagawa, S., Tap, J., Tims, S., Zoetendal, E. G., Brunak, S., Clément, K., Doré, J., Kleerebezem, M., Kristiansen, K., Renault, P., Sicheritz-Ponten, T., Vos, W. M., Zucker, J.-D., Raes, J., Hansen, T., Bork, P., Wang, J., Ehrlich, S. D., & Pedersen, O. (2013). Richness of human gut microbiome correlates with metabolic markers. *Nature*, 500(7464), 541-546. http://dx.doi.org/10.1038/nature12506. PMid:23985870.

Cheng, M., Zhang, X., Miao, Y., Cao, J., Wu, Z., & Weng, P. (2017). The modulatory effect of (-)-epigallocatechin 3-O-(3-O-methyl) gallate (EGCG3 ″Me) on intestinal microbiota of high fat diet-induced obesity mice model. *Food Research International*, 92, 9-16. http://dx.doi.org/10.1016/j.foodres.2016.12.008. PMid:28290302.

Cho, K. W., Kim, Y. O., Andrade, J. E., Burgess, J. R., & Kim, Y. (2011). Dietary naringenin increases hepatic peroxisome proliferators–activated receptor α protein expression and decreases plasma triglyceride and adiposity in rats. *European Journal of Nutrition*, 50(2), 81-88. http://dx.doi.org/10.1007/s00394-010-0117-8. PMid:20567977.

Cicchese, J. M., Evans, S., Hult, C., Joslyn, L. R., Wessler, T., Millar, J. A., Marino, S., Cilfone, N. A., Mattila, J. T., Linderman, J. J., & Kirschner, D. E. (2018). Dynamic balance of pro-and anti-inflammatory signals controls disease and limits pathology. *Immunological Reviews*, 285(1), 147-167. http://dx.doi.org/10.1111/imr.12671. PMid:30129209.

Coronado-Reyes, J. A., Cortés-Penagos, C. D. J., & González-Hernández, J. C. (2022). Chemical composition and great applications to the fruit of the pomegranate (Punica granatum): a review. *Food Science and Technology*, 42, e29420. http://dx.doi.org/10.1590/fst.29420.

Demizieux, L., Piscitelli, F., Troy-Fioramonti, S., Iannotti, F. A., Borrino, S., Gresti, J., Muller, T., Bellenger, J., Silvestri, C., Marzo, V., & Degrace, P. (2016). Early low-fat diet enriched with linolenic acid reduces liver endocannabinoid tone and improves late glycemic control after a high-fat diet challenge in mice. *Diabetes*, 65(7), 1824-1837. http://dx.doi.org/10.2337/db15-1279. PMid:27207550.

Harzallah, A., Hammami, M., Kępczyńska, M. A., Hislop, D. C., Arch, J. R. S., Cawthorne, M. A., & Zaibi, M. S. (2016). Comparison of potential preventive effects of pomegranate flower, peel and seed oil on insulin resistance and inflammation in high-fat and high-sucrose diet-induced obesity mice model. *Archives of Physiology and Biochemistry*, 122(2), 75-87. http://dx.doi.org/10.3109/13813455.2016.1148053. PMid:26822470.

Hou, Q., Zhao, F., Liu, W., Lv, R., Khine, W. W. T., Han, J., Sun, Z., Lee, Y., & Zhang, H. (2020). Probiotic-directed modulation of gut microbiota is basal microbiome dependent. *Gut Microbes*, 12(1), 1736974. http://dx.doi.org/10.1080/19490976.2020.1736974. PMid:32200683.

Kim, B., Choi, H., & Yim, J. (2019). Effect of diet on the gut microbiota associated with obesity. *Journal of Obesity & Metabolic Syndrome*, 28(4), 216-224. http://dx.doi.org/10.7570/jomes.2019.28.4.216. PMid:31909364.

Liu, P., Liu, M., Liu, X., Xue, M., Jiang, Q., & Lei, H. (2022). Effect of alpha-linolenic acid (ALA) on proliferation of probiotics and its adhesion to colonic epithelial cells. *Food Science and Technology*, 42, e71921. http://dx.doi.org/10.1590/fst.71921.

Lozupone, C. A., Stombaugh, J. I., Gordon, J. I., Jansson, J. K., & Knight, R. (2012). Diversity, stability, and resilience of the human gut microbiota. *Nature*, 489(7415), 220-230. http://dx.doi.org/10.1038/nature11550. PMid:22972295.

Mi, S., Gu, J., Cao, X., Li, Y., Xu, Q., Chen, W., & Zhang, Y. (2022). Regulatory mechanism of fermented wheat germ on lipid metabolism

in hyperlipidemia rats via activation of AMPK pathway. *Food Science and Technology*, 42, e57222. http://dx.doi.org/10.1590/fst.57222.

Rachid, T. L., Silva-Veiga, F. M., Graus-Nunes, F., Bringhenti, I., Mandarim-de-Lacerda, C. A., & Souza-Mello, V. (2018). Differential actions of PPAR-α and PPAR-β/δ on beige adipocyte formation: a study in the subcutaneous white adipose tissue of obese male mice. *PLoS One*, 13(1), e0191365. http://dx.doi.org/10.1371/journal.pone.0191365. PMid:29351550.

Raffaele, M., Licari, M., Amin, S., Alex, R., Shen, H., Singh, S. P., Vanella, L., Rezzani, R., Bonomini, F., Peterson, S. J., Stec, D. E., & Abraham, N. G. (2020). Cold press pomegranate seed oil attenuates dietary-obesity induced hepatic steatosis and fibrosis through antioxidant and mitochondrial pathways in obese mice. *International Journal of Molecular Sciences*, 21(15), 5469. http://dx.doi.org/10.3390/ijms21155469. PMid:32751794.

Shagholian, M., Goli, S. A. H., Shirvani, A., Agha-Ghazvini, M. R., & Asgary, S. (2019). Liver and serum lipids in Wistar rats fed a novel structured lipid containing conjugated linoleic acid and conjugated linolenic acid. *Grasas y Aceites*, 70(2), 307. http://dx.doi.org/10.3989/gya.0582181.

Szymczyk, B., & Szczurek, W. (2016). Effect of dietary pomegranate seed oil and linseed oil on broiler chickens performance and meat fatty acid profile. *Journal of Animal and Feed Sciences*, 25(1), 37-44. http://dx.doi.org/10.22358/jafs/65585/2016.

Turnbaugh, P. J., Ley, R. E., Mahowald, M. A., Magrini, V., Mardis, E. R., & Gordon, J. I. (2006). An obesity-associated gut microbiome with increased capacity for energy harvest. *Nature*, 444(7122), 1027-1031. http://dx.doi.org/10.1038/nature05414. PMid:17183312.

Walters, W. A., Xu, Z., & Knight, R. (2014). Meta-analyses of human gut microbes associated with obesity and IBD. *FEBS Letters*, 588(22), 4223-4233. http://dx.doi.org/10.1016/j.febslet.2014.09.039. PMid:25307765.

Wang, L., Zhang, Y., Fan, G., Ren, J. N., Zhang, L. L., & Pan, S. Y. (2019). Effects of orange essential oil on intestinal microflora in mice. *Journal of the Science of Food and Agriculture*, 99(8), 4019-4028. http://dx.doi.org/10.1002/jsfa.9629. PMid:30729524.

Wu, L., Tang, B., Lai, P., Weng, M., Zheng, H., Chen, J., & Li, Y. (2022). Analysis of the effect of okra extract on the diversity of intestinal flora in diabetic rats based on 16S rRNA sequence. *Food Science and Technology*, 42, e00121. http://dx.doi.org/10.1590/fst.00121.

Xu, X.-R., Liu, C.-Q., Feng, B.-S., & Liu, Z.-J. (2014). Dysregulation of mucosal immune response in pathogenesis of inflammatory bowel disease. *World Journal of Gastroenterology*, 20(12), 3255-3264. http://dx.doi.org/10.3748/wjg.v20.i12.3255. PMid:24695798.

Yoo, J. Y., Groer, M., Dutra, S. V. O., Sarkar, A., & McSkimming, D. I. (2020). Gut microbiota and immune system interactions. *Microorganisms*, 8(10), 1587. http://dx.doi.org/10.3390/microorganisms8101587. PMid:33076307.

Yuan, G. F., Chen, X. E., & Li, D. (2014). Conjugated linolenic acids and their bioactivities: a review. *Food & Function*, 5(7), 1360-1368. http://dx.doi.org/10.1039/c4fo00037d. PMid:24760201.

Zacarías, M. F., Collado, M. C., Gómez-Gallego, C., Flinck, H., Aittoniemi, J., Isolauri, E., & Salminen, S. (2018). Pregestational overweight and obesity are associated with differences in gut microbiota composition and systemic inflammation in the third trimester. *PLoS One*, 13(7), e0200305. http://dx.doi.org/10.1371/journal.pone.0200305. PMid:30005082.

Zhang, M., Du, N., Wang, L., Wang, X., Xiao, Y., Zhang, K., Liu, Q., & Wang, P. (2017). Conjugated fatty acid-rich oil from Gynostrmma pentaphyllum seed can ameliorate lipid and glucose metabolism in type 2 diabetes mellitus mice. *Food & Function*, 8(10), 3696-3706. http://dx.doi.org/10.1039/C7FO00712D. PMid:28944807.

Zou, Y., Yu, H., Zhang, L., & Ruan, Z. (2021). Dietary vegetable powders modulate immune homeostasis and intestinal microbiota in mice. *Foods*, 11(1), 27. http://dx.doi.org/10.3390/foods11010027. PMid:35010153.